ISSN 1995-0780, Nanotechnologies in Russia, 2016, Vol. 11, Nos. 9–10, pp. 593–602. © Pleiades Publishing, Ltd., 2016.
Original Russian Text ©A.A. Kuzharov, A.A. Milov, U.S. Gerasina, H. Nguyen, A.V. Tischenko, K.A. Lomachenko, A.V. Soldatov, 2016, published in Rossiiskie Nanotekhnologii, 2016, Vol. 11, Nos. 9–10.

# Nanotribology of Copper Clusters

**A. A. Kuzharov[a]*, A. A. Milov[b], U. S. Gerasina[a], H. Nguyen[a], A. V. Tischenko[a], K. A. Lomachenko[c], and A. V. Soldatov[c]**

[a] *Don State Technical University, Rostov-on-Don, 344000 Russia*
[b] *Southern Scientific Center, Russian Academy of Sciences, Rostov-on-Don, 344006 Russia*
[c] *Southern Federal University, Rostov-on-Don, 344006 Russia*
**e-mail: akuzharov@gmail.com*

Received February 7, 2016; in final form, June 14, 2016

**Abstract**—The use of nanotechnologies in tribology has led to a large number of marketable lubricants containing nanoparticles with unproven efficiency. Tribological and physicochemical studies of some lubricant additives aimed at determining the tribological characteristics are presented in this work. It is found that applying metal particles (copper, above all) may lead to increased tribotechnical characteristics of lubricants. The quantum chemical calculations with the full optimization of all parameters by the method of the density functional theory (DFT) PBEPBE/Lanl2DZ were carried out in order to identify the mechanism of formation and growth of copper nanoclusters as a modeling basis of the metal-clad component of the tribosystems. It is shown that the formation of Cu nanoparticles and their shape are related with the growth of nanoclusters, their stabilization by ligands, and their aggregation, as well as agglomeration and coalescence, which results in nanoparticles of sizes ranging from a few to tens and hundreds of nanometers of different shapes. The synthesis of copper nanoclusters aimed at studying physical and chemical characteristics and their application as functional tribological nanomaterials is carried out. The efficiency of such lubricant compositions is determined.

**DOI:** 10.1134/S1995078016050104

## INTRODUCTION

The extensive use of nanotechnologies in different areas of science and technology could not pass by such an important domain of science as tribology. In this case the nanotechnological approach is implemented in molecular tribology and nanotribology which studies and describes the tribological effects in the nanoscale. First and foremost it is connected with studies carried out with the use of the atomic force microscopes [1, 2], making it possible to register atomic interactions in the tribosystems. It is necessary to mention here that almost always there is "dry" friction between the probe of the atomic force microscopes and atomically smooth surfaces. Such studies are certainly important for understanding the friction mechanisms on nanocontact, and that may be useful in the future for explaining the tribological processes of the frictional interaction in micro- and macroranges; however they are quite far from friction in acting systems. In our mind, the application of nanotechnologies in nanotribology shall not be restricted by the use of extremely precise and sensitive test procedures on the nanoscale, but it shall involve the application of nanomaterials as additives to the lubricants aiming at providing higher tribological effects in comparison with micro- and macrometerials. Of course, the application of nanoparticles [3], especially metals [4–9], is a common event and even almost universal. For example, the modern market of automotive lubricants is peppered with various "miraculous" nanoadditives [10, 11] that critically change the properties of the friction contact and considerably increase the service life of combustion engines or transmissions. However, most often this is no more than false advertising: either the particles are not of a nanoscale, the materials do not correspond to the advertised ones, or the effect is not as prominent (if there is any effect at all). There is no question of the scientific approach connected with the study of the building mechanism or lubricating effect of nanoparticles, determining the optimum concentrations or compositions, and (perhaps most importantly) determining dimensional tribological effects after nanomaterial application. In reference with the above, this work makes attempts to consider some aspects of the tribological use of nanomaterials and nanoparticle building mechanisms and study their influence on the lubrication mechanism.

## EXPERIMENTAL

Marketable additives for engine oils meant for improving the service properties of automotive engine and transmission oils were used as study objects: Metalyz-6, Nano Doctor, Plamet, R1Metall, R1Metall-T,

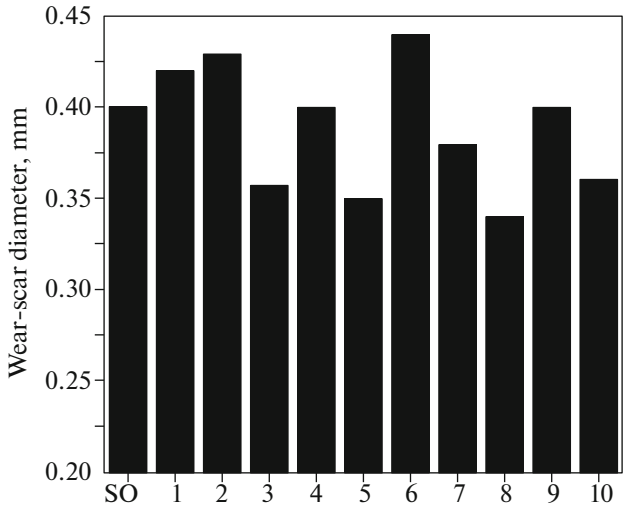


**Fig. 1.** Wear preventive properties of the lubricant compositions during testing on FBM: (1) SO, (2) SO + Metalyz-6, (3) SO + Nano Doctor, (4) SO + Plamet, (5) SO + R1Metall, (6) SO + R1Metall-T, (7) SO + Restore, (8) SO + Resurs, (9) SO + Resurs-T, (10) SO + RiMET-100, and (11) SO + RiMET-Nano.

Restore, Resurs, Resurs-T, RiMET-100, and RiMET-Nano. Additives were introduced into Castrol Magnatec 5w-40 C3 synthetic oil (SO) with bulk concentrations recommended by manufacturer.

Obtaining copper nanoparticles involves the electrochemical dilution of a copper anode and the recovery of copper ions on the cathode in the stabilizer solution and under the ultrasonic influence. Water solutions with the addition of a stabilizer, gelatin, were used as the electrolytes during electrolyze. Electrodes were made from metal, with the minimum concentration of additives. The process took place under different current densities (6, 9, and 12 mA/cm$^2$) and stabilizer amounts (0.5, 1.0, and 1.5% by mass). Then the sols were dried.

The chemical composition of the metal-clad components of the additives was carried out by X-ray fluorescence analysis (XFA) with a Spectroscan MAKC-GV portable vacuum spectrometer in a solid state after extracting metal particles from suspension matters, washing by hexane, and drying.

Comparison tribological tests of the lubricating materials were carried out with the four-ball machine (FBM) according to GOST 9490-75 (ASMT D2783) using Ø ½" balls made of ShX-15 steel; wear-scar diameter ($D_w$) under different loads and time of the frictional interaction, critical load ($P_c$), welding load ($P_w$), and load wear index ($I_{lw}$) were used as the estimated figures.

The shape and size of nanoparticles were tested with a PHYWE atomic force microscope in the semi-contact mode and with a Microtrac NANO-flex laser analyzer by the dynamic light scattering method.

Quantum chemical calculations were made with the full optimization of all parameters by the DFT method PBEPBE/Lanl2DZ using the package of the Gaussian 09 program [12]. Identification of the stationary points was carried out by the calculation of the force constant matrix. All given structures are minimums on the corresponding potential energy surfaces (PES).

## RESULTS AND DISCUSSIONS

In order to reveal potentials of lubricating materials containing metal-clad components including nanomaterials, as claimed by manufacturers, the physicochemical and tribological properties of additives to engine oils presented on the modern automobile chemistry market were studied. Tests results carried out with FBM at P = 392 H within 3600 seconds demonstrate that additives in SO (excluding Plamet, R1Metall-T, Resurs-T, and RiMET-Nano) exert insignificant influence on the antiwear characteristics (wear-scar diameter $D_w$ (Fig. 1)) of the lubricant bases. The introduction of some additives results in a deterioration of the antiwear characteristics of the base oil, for example, Metalyz-6, Nano Doctor, and Restore.

It is also necessary to mention that introducing additives into SOs, except for Nano Doctor, which deteriorates the scoring resistance of the lubricant base, does not exert an influence on the scoring resistance of the base (Fig. 2).

The studies of the bearing strength and ultimate load of the lubricant (Fig. 3) demonstrate that the introduction of additives into the SO improves the ultimate bearing strength of the base. For example, the R1Metall-T and Resurs-T additives show the 1.5 increase of the welding load ($P_w$) against the oil without additives. However the introduction of additives into the SO does not result in a noticeable increase in the lubricant bearing strength. The difference of the pure SO from oil-containing market-grade additives is not significant.

Thus, the introduction of additives to the lubricant is by far not as clear-cut as is claimed by manufacturers and by no means always shows a positive effect. Nevertheless, in some cases, such additives may improve the tribotechnical characteristics of the frictional contact, but in a minor way.

The influence of the elemental constituents of the metal-cladding components on the tribotechnical properties of the lubricant compositions was made with the help of an X-ray fluorescence analysis (XFA) of the studied additives (Table); analysis showed that the base for all market-grade products is copper, which is a classic metal-clad functional material providing the recovery of the IC engines moving parts.

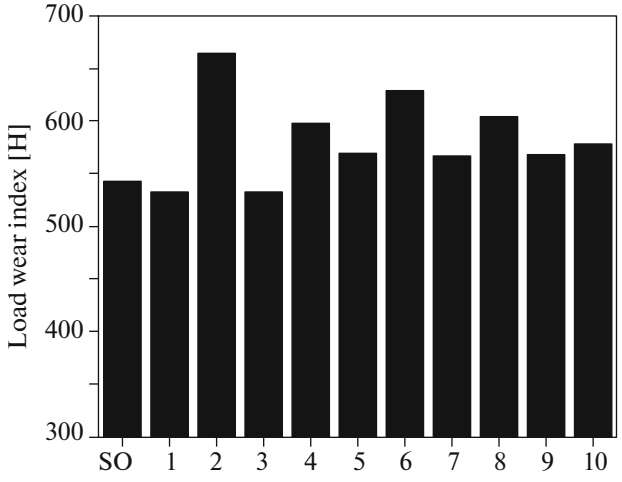


**Fig. 2.** Scoring resistance of the lubricant compositions during a test on the FBM: (1) SO + Metalyz-6, (2) SO + Nano Doctor, (3) SO + Plamet, (4) CM + R1Metall, (5) SO + R1Metall-T, (6) SO + Restore, (7) SO + Resurs, (8) SO + Resurs-T, (9) SO + RiMET-100, and (10) SO + RiMET-Nano.

Some elements, Ag for example, indicated by some manufacturers, were not found in the compositions.

An analysis of sizes by dynamic light scattering showed that additives contain particles in a wide range of size distribution: from tens of nanometers to the micrometer range; in some cases, that allowed technically to position these products as nanotechnology products.

Based on the above, it may be stated that the application of high dispersive metal particles (copper primarily) may lead to an increase in the tribotechnical characteristics of the lubricating materials. However, the influence of size and shapes of the metal particles and mechanism of their formation, as well as the connection between these physicochemical characteristics and tribological properties of the tribological systems, are not properly studied or not studied at all as of today.

Quantum chemical calculations with full optimization of all parameters by the method of the density functional theory ((DFT) PBEPBE/Lanl2DZ) were made in order to define the mechanism of formation and growth of the copper nanoclusters as the model tribotechnical base of the metal-cladding component of the tribological systems.

As was shown in [13], for the 13-atomic copper cluster, the icosahedral structure is more stable against cuboctahedral configuration indicative for the massive copper; that is why the study of the growth connected with layer growth of the copper cluster was carried out on the basis of the icosahedral systems.

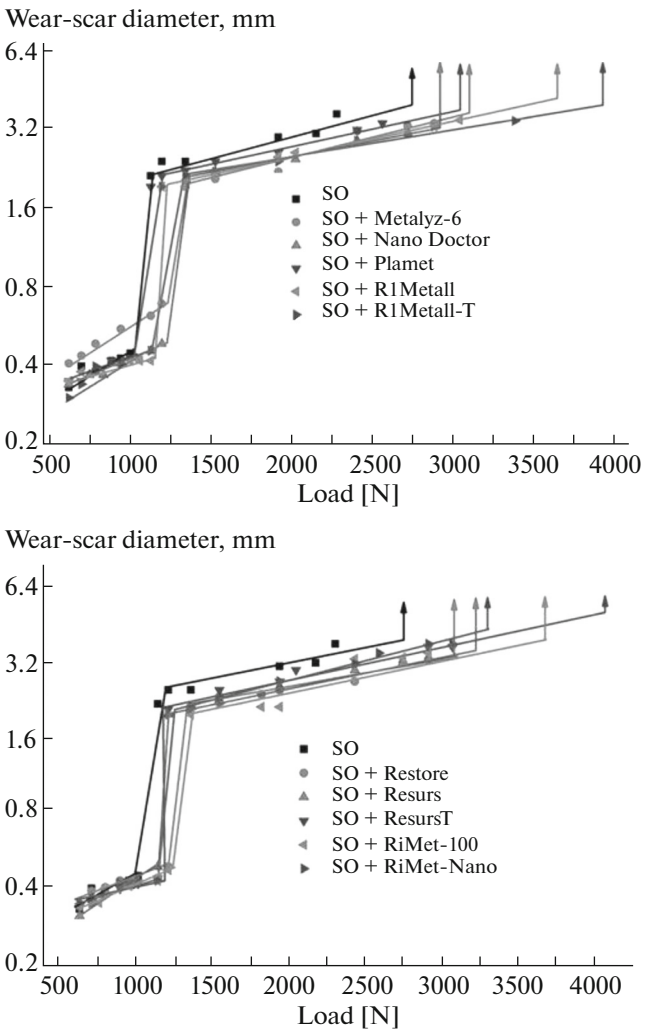


**Fig. 3.** Dependence of the wear-scar diameter on the load at 10-s test on the FBM.

Thus, with the help of calculations, the process of the cluster layerwise increase with the maximum symmetry retention was studied in the following sequence: $Cu_1 \rightarrow Cu_{13} \rightarrow Cu_{33} \rightarrow Cu_{45}$. The transition from structure to structure was as follows: during $Cu_1 \rightarrow Cu_{13}$ transition, the copper atom (center) was encircled by 12 copper atoms in the icosahedral symmetry; the $Cu_{13} \rightarrow Cu_{33}$ transition was fulfilled by the placement of every three-angle side of the 13 atomic symmetric cluster of the new copper atom with the formation of the trigonal pyramid on the symmetry axis.

The $Cu_1 \rightarrow Cu_{13}$ transition leads to icosahedral structure 1 and reflects the formation of the first spherical-symmetry layer around the copper atom (Fig. 4). Calculations show that the distance between the copper central atom and any atom on the cluster surface $Cu_{13}$ is about 2.48 Å, and the radius of the corresponding Onsager sphere is 5.11 Å. The analysis of

Results of a quantitative analysis of the metal-clad components of the remetallizers and their wear preventive properties

| Additives | Elemental constituents, % | | | | | | | | |
|---|---|---|---|---|---|---|---|---|---|
| | Ca | Cu | Fe | Ni | P | Pb | S | Sn | Zn |
| Metalyz-6 | 2.1 | 85.5 | – | – | 0.65 | 10.2 | 1.5 | – | – |
| Nano Doctor | 0.76 | 87.7 | 0.19 | 10.3 | 0.16 | – | 0.16 | – | |
| Plamet | 8.9 | 73.2 | 0.55 | – | 0.59 | – | 8.87 | – | 3.6 |
| R1Metall | – | 93.2 | – | – | 0.2 | – | 0.15 | 6.2 | – |
| R1Metall-T | – | 84.2 | 0.1 | – | 0.36 | – | 1.7 | 3.64 | – |
| Restore | 5.8 | 42.4 | 0.22 | – | – | 51.3 | 0.25 | – | – |
| Resurs | – | 92.9 | – | – | 0.16 | – | 0.22 | 6.5 | – |
| Resurs-T | – | 78.1 | 0.12 | 2.5 | 0.81 | – | 0.87 | 3.2 | 14 |
| RiMET-100 | – | 94.4 | – | – | – | – | – | 5.6 | – |
| RiMET-Nano | 8.67 | 84.5 | – | – | 0.07 | – | 0.18 | 3.1 | – |

the natural bond orbitals (NBOs) shows a significant division of charges between central and boundary copper atoms: the central atom bears a negative charge and the boundary of the cluster possesses some deficit of the electronic density ~0.1 e in each center.

The addition of one copper atom to structure 1 leads first to 14 atomic isomer 2 with the noticeable distortion icosahedral frame (Fig. 4): for cluster 1 the distance to the copper atoms on the surface was 2.48 Å, and in structure 2 those distances show changes within 2.30–2.93 Å (the distance from the center to the 14 copper atom is 4.20 Å); the growth of the Onsager sphere radius as compared to the structure 1 is 0.19 Å and shows 5.30 Å. Structure 2 is not minimal on the PES and isomerizes into form 3 (Fig. 5), presenting two uncompleted icosahedral fragments. This structure has the dipole moment 0.36D; its direction is shown in Fig. 5 and all the intercenter Cu-Cu distances are within the 2.4–2.6 Å range indicative of the 13 atomic icosahedral cluster. It is required to mention that, based on the NBO analysis, the centers of the uncompleted clusters bear the negative charge ~0.8–1.0 e, and the radius of the Onsager sphere is 5.50 Å, which is 0.3 Å more when compared for structure 2. Thus, progressive structures—but not the spherical ones—will be found under the constant

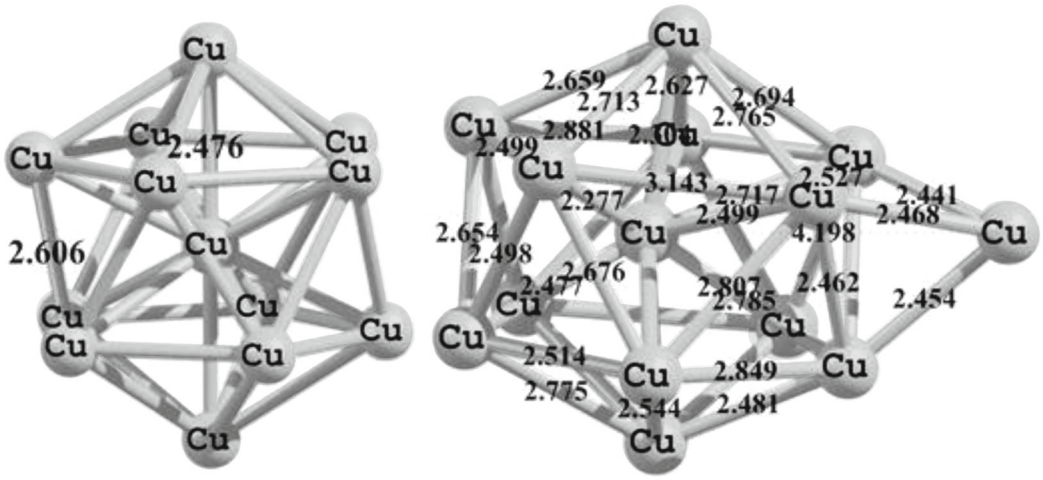


**Fig. 4.** Geometry features of clusters **1** and **2**. All lengths are given in angstroms.

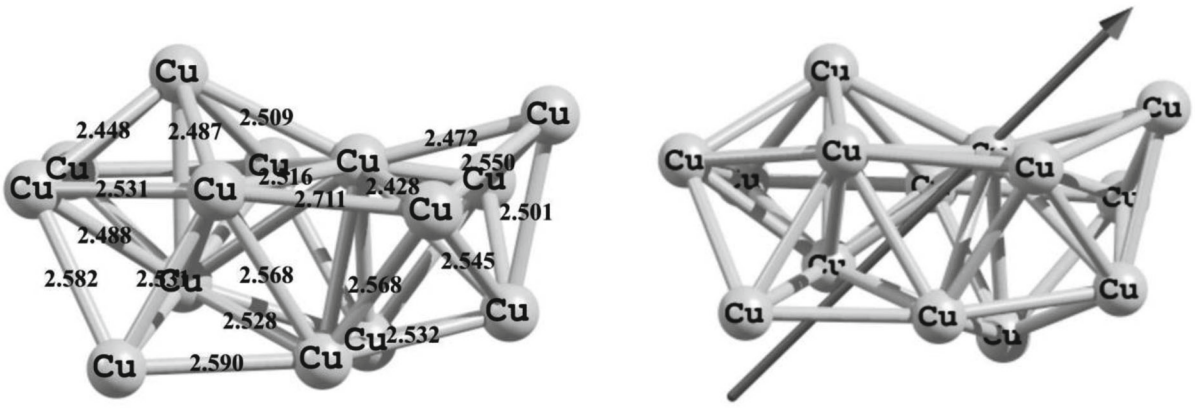


**Fig. 5.** Geometry feature and dipole moment of cluster **3**.

growth of the copper cluster. Such a situation will be escalated in the case of field overlapping due to the polarity of the received clusters.

During $Cu_{13} \rightarrow Cu_{33}$ transition, we shall get the structure 4 (Fig. 7); in this structure the internal $Cu_{13}$ fragment is practically not changed when compared to the initial $Cu_{13}$ cluster. The second layer of atoms forms up in such manner that it forms the pentagonal pyramid on the nodes of the initial icosahedron; the top of the pyramid is one of the atoms of the copper first layer, as is shown in Fig. 6. The distance from the center of cluster 4 to the copper atoms of the first layer is 2.50–2.58 Å; the distance from the copper central atom to the atoms of the second layer is 3.89–4.02 Å. The radius of the Onsager sphere of structure 4 is 6.48 Å (Fig. 7).

The $Cu_{33} \rightarrow Cu_{45}$ transition was carried out by the scheme shown in Fig. 8: each fragment of the $Cu_{33}$ cluster surface corresponding to the pentagonal pyramid is built up to the bipyramid. An elongated system of cylindrical shape, structure 5, instead of a spherical particle, is obtained (Fig. 9). As is seen, the distance between the outermost atoms of cluster 5 along the axis of the cylinder is ~9.0 Å and the radius of the cylinder is ~8.0 Å; that corresponds to the distances between the outermost atoms of the $Cu_{33}$ cluster. Thus, a certain aptitude to the unidirectional cluster size growth, out of three of them, is observed. The distance from the cluster center to the third layer of the copper atoms changes within 4.68–4.79 Å, to the second layer it is 3.95–4.00 Å, and to the atoms of the first layer it is 2.34–2.48 Å; that shows some tendency to the compression of the first atomic layer and elongation of the second layer under the influence of the third layer of the metal atoms. The radius of the Onsager sphere is 7.34 Å.

Because the existence of clusters nonstabilized by ligands is practically not possible in actual practice, the influence of solvation on the structure of the copper clusters was studied with the help of organic stabilizers and water molecules added to the $Cu_{13}$ and $Cu_{33}$ clusters. Thus, $Cu_1 \cdot H_2O$ (**6**), $Cu_{13} \cdot 12H_2O$ (**7**), $Cu_{13} \cdot 22H_2O$ (**8**), $Cu_{13} \cdot 12EtOH$ (**9**), and $Cu_{33} \cdot 20EtOH$ (**10**) structures were studied.

Calculations showed that coordination of one water molecule on the surface of the $Cu_{13}$ cluster rebuilt the whole system of the copper cluster, but negligibly (Fig. 10). Thus, in structure 6, the central atom of the cluster is ~0.10 Å closer to the copper atom to which the water molecule is attached; the contact length of the central cluster atom with the copper atom located on the same axis as the coordination center shortens by ~0.05 Å, and the rest of the lengths of the Cu-Cu contacts increase. Thus, the deformation of the copper cluster induced by the bonding of one water

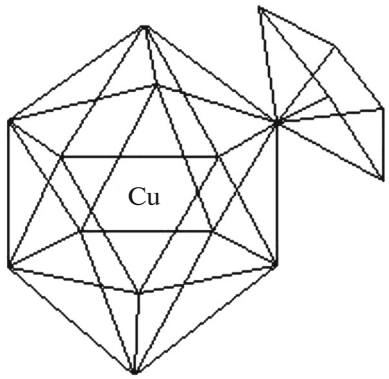


**Fig. 6.** Formation pattern of the copper atoms new layer of the $Cu_{13}$ icosahedron.

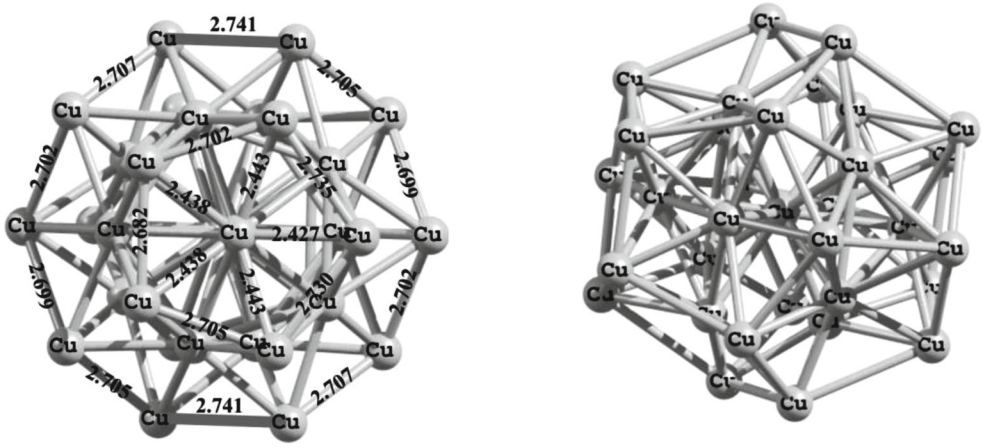


**Fig. 7.** Geometry features of cluster **4.**

molecule resembles the elastic collision of two spherical bodies; at that, the length of the Cu-O contact is 2.016 Å. A similar change in the icosahedral structure is obtained after the introduction of the 12 water molecules (structure 7). It is clear that 12 water molecules are not enough for the uniform envelopment of the whole copper cluster surface; that is why deformational changes, when compared with the gas-phase $Cu_{13}$ structure, are more noticeable. The Cu-O distance for all contacts is increased by ~0.1 Å. It is clear that with a small amount of water molecules the copper cluster will be considerably closer to its ideal structure, but with increased distances from the central copper atom to the periphery.

The calculation shows that, with the increase of some water molecules up to 26 molecules (structure 8), the deformation of the $Cu_{13}$ icosahedral structure becomes considerably lower. Thus, in the case with the $Cu_{13} \cdot 12H_2O$ cluster, the distance between copper atoms on the cluster surface changes within 2.5–2.9 Å and with the $Cu_{13} \cdot 26H_2O$ cluster those distances change within 2.5–2.7 Å; the distance from the cluster center to the surface atoms changes within 2.4–2.6 Å. That is quite close to the parameters of the nondistorted icosahedral system. The radius of the Onsager sphere for the $Cu_{13} \cdot 26H_2O$ structure is 6.77 Å. Thus, the growth of the water molecules on the surface of the copper cluster strongly deforms its structure at the beginning, but with some amount of water molecules it starts contributing to its symmetrical organization.

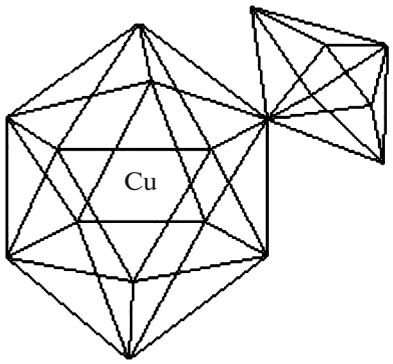


**Fig. 8.** Formation pattern of the copper atoms new layer of the $Cu_{33}$ icosahedron.

Contrary to water molecules, the 12 ethanol molecules (structure 9) interact with the copper cluster in such manner that it does not deform its structure; its bonds length is close to the ideal icosahedral structure (Fig. 11). This fact is mainly connected with the size of the alcohol molecules, which are appreciably larger than the water molecules. It is necessary to mention that the Cu-O for ethanol is 2.15–2.20 Å and that is at least 0.1 Å higher than for the water molecules.

At the same time, in the $Cu_{33} \cdot 20EtOH$ (structure 10), the central copper cluster increases its Cu-Cu bonds but preserves its spatial structure.

As is seen from the above calculations, the growth of nanoparticles is connected with the layerwise growth of copper clusters and their further stabilization: that leads to the formation of nanoparticles in a wide size range from ~0.5 nm (minimal for $Cu_{13}$). The possible shape of the nanoparticles is also varied: from spherical and cylindrical to asymmetrical and absolute anisodiametry. The formation of nanoparticles and their shape are connected not only with the growth of nanoclusters and their stabilization, but with their aggregation, agglomeration, and coalescence; that may result in the formation of nanoparticles from several to tens and hundreds nanometers of various shapes.

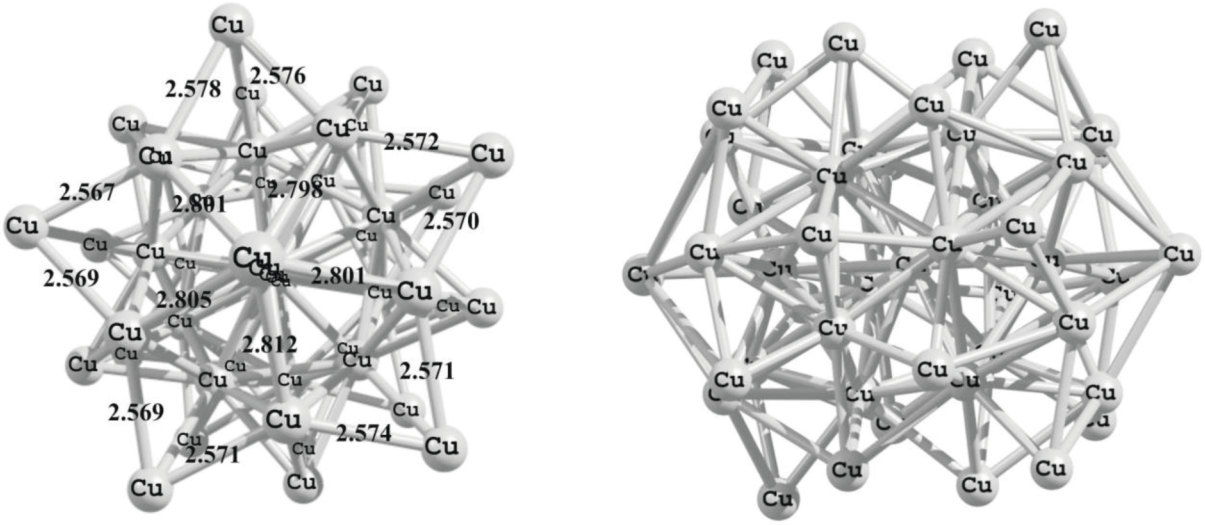

**Fig. 9.** Geometry features of cluster **5**.

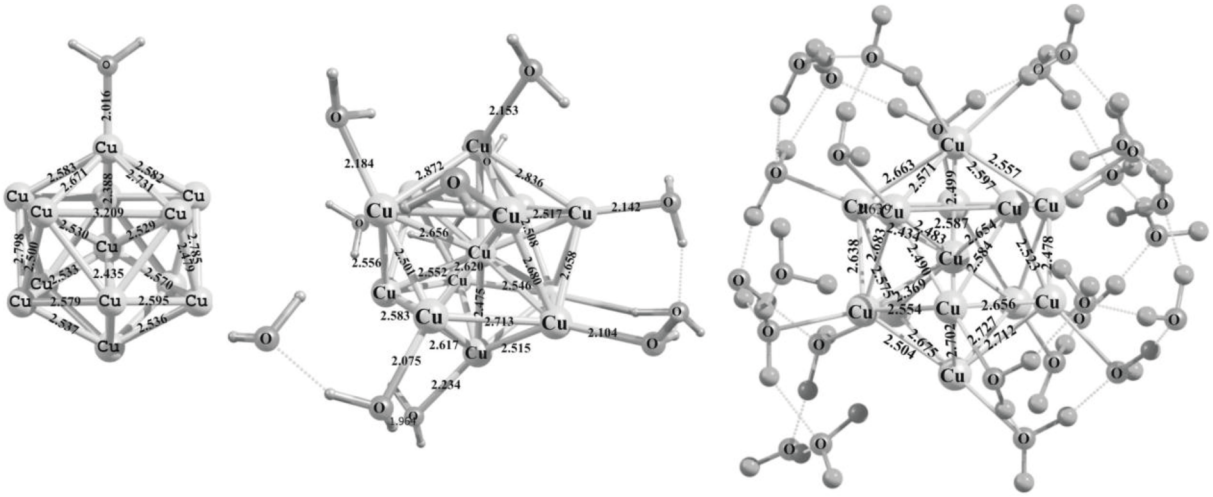

**Fig. 10.** Geometry features of clusters **6** ($Cu_{13} \cdot H_2O$), **7** ($Cu_{13} \cdot 12H_2O$), and **8**($Cu_{13} \cdot 26H_2O$).

Synthesis of the nanoscale copper clusters by combined sound-electrochemical technology was made on the basis of quantum chemical calculations for their further application as functional nanomaterials for tribotechnical use. The study of synthesized copper nanoparticles by dynamic light scattering showed that the copper nanomaterials include the distribution of nanoparticles by size from several tens of nanometers to several hundred nanometers, depending on synthesis conditions. It was found that, based on the spatial distribution of particles, for example, Fig. 12, a variation in technological parameters (density of the electrolyze current, power of the US impact, and some stabilizers) may help getting nanoparticles with different sizewise distributions of particles starting from several tens of nanometers. Samples obtained at average values of the current density, 10 mA/cm$^2$ and minimal concentration of stabilizer, 0.5% by mass, possesses the smallest sizes.

Atomic force microscopy (AFM) was used to support the results of dynamic light scattering and reveal shapes of the copper nanoparticles. It was proved that the synthesized nanoclusters have sizes of no less than 100 nm and are aniso-diametric particles (Fig. 13) in the form of the different ellipsoids. The formation of such particles is likely to be connected with the fact that, at the beginning, copper nanoparticles similar in shape to spherical ones are formed on the cathode sur-

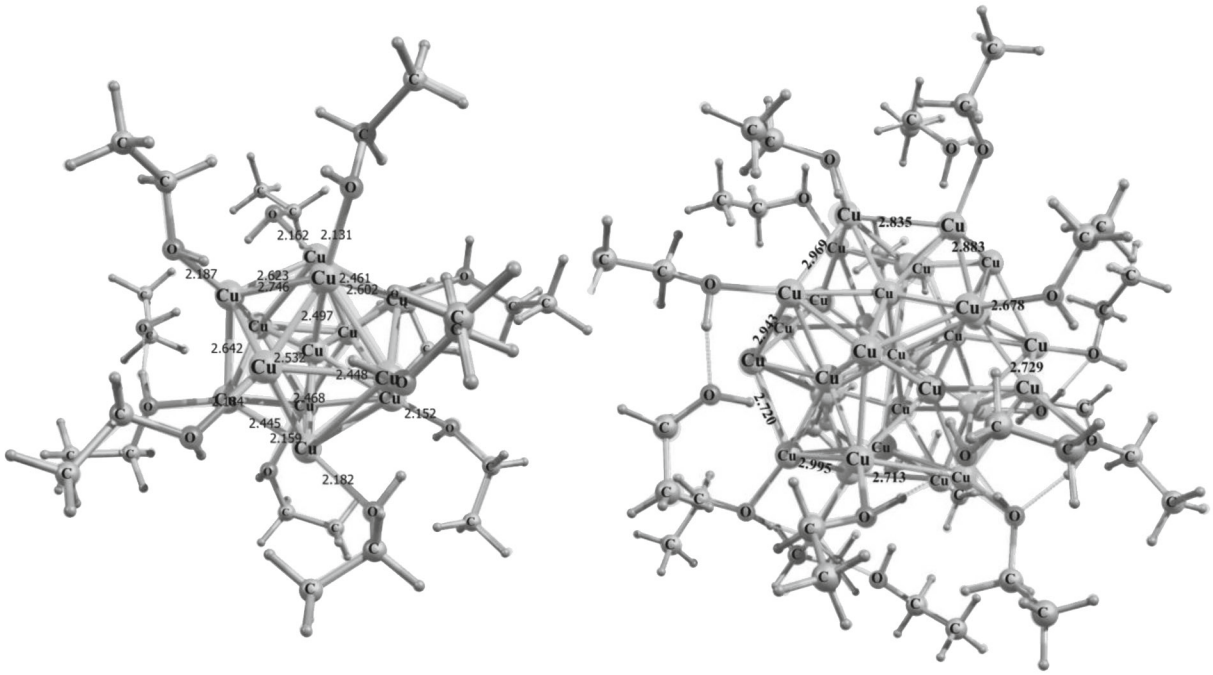

**Fig. 11.** Structure of clusters **9** ($Cu_{13}$ • 12EtOH) and **10** ($Cu_{33}$ • 20EtOH).

face; they are poorly connected with the cathode surface, which is why they may be easily detached from its surface by ultrasonic or cavitation impact. In the future, the nanoparticles, being in close proximity, become bigger, coalescent, and may form clusters not only of the spherical form, but in the form of the different ellipsoids, due to aggregation; that is clearly seen on the AFM image. The following situation is possible: the cylindrical shape of the nanoparticles may be connected with the immediate growth of the copper clusters, as was proven by the above quantum-chemical calculations. The equivalent volume of the obtained nanoparticles corresponds to a radius sphere

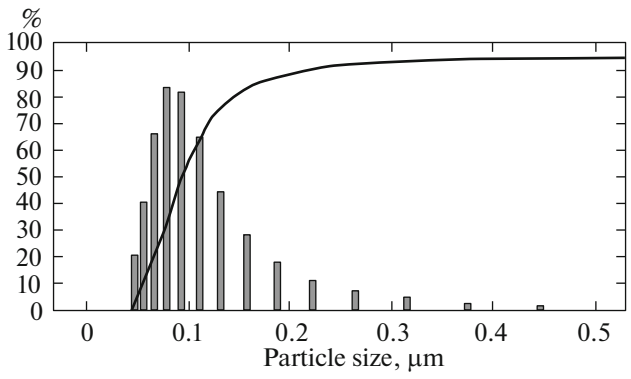


**Fig. 12.** Distribution of the copper nanoparticles by sizes.

of 30–40 nm; that is well coordinated with the dynamic light scattering data showing the initial size of copper clusters being the base for bigger nanoparticles. Based on the quantum chemical calculations, it may be claimed that at the first moment the "ideal" nanoclusters of the icosahedral $Cu_{13}$shape of no less than 1 nm size are formed on the electrode surface; in the future they may either coalesce, form new bigger ellipsoid nanoparticles, or continue to grow up to $Cu_{33}$ or $Cu_{45}$ (changing their shape to more complex or anisodiametrical particles). That results in their further coalescent and aggregation. Parallel to the above, those particles "herd together" in liquid medium under the ultrasonic impact and cavitation; that takes place due to their stabilization by molecules of stabilizer, resulting in the further growth of the particle size and allows one to allocate nanoparticles of several tens of nanometers and more from the reaction medium.

A test on the FBM equipment was made to evaluate the tribotechnical possibilities of the copper nanoclusters as part of the lubricants. Glycerin was applied as the lubricant base because it has low tribotechnical characteristics and is a classical lubricant base. Samples of the copper nanopowders were used as additives; the concentration was 2.5, 5, and 10% by mass.

Results of tribological tests (Fig. 14) showed that the introduction of the copper nanoparticles into the lubricant media exerted a positive influence on the tribological characteristics of the basic lubricant—glyc-

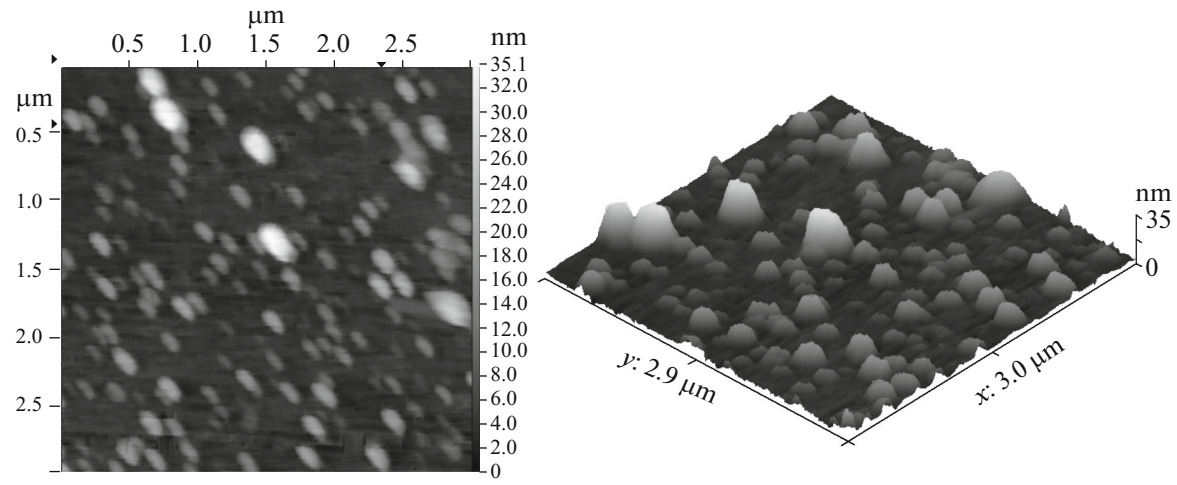


**Fig. 13.** AFM image of the copper nanoclusters.

erin; it results in a decrease in the wear-scar diameter. Thus, the most wear decrease, by 33%, is indicative for the compositions containing 70 nm of the copper nanoparticles. This shows that the lubricant contains a sufficient amount of the metal-cladding component; the formation of the protective copper (servovite film) takes place in a certain friction moment, after saturation of the moving surfaces by the copper nanoparticles, allowing for the effective decrease in the wear values.

Considering the influence of the average size of copper nanoparticles on the tribological properties of the lubricant media (Fig. 14), it is necessary to mention that, other conditions being equal, the size decrease of the copper particles added to the lubricant composition leads to an increase in the antiwear properties of the tribocoupling; that is manifested by the decrease in the wear-scar diameter during FBM tests when compared to the basic lubricant without the introduction of the nanoparticles.

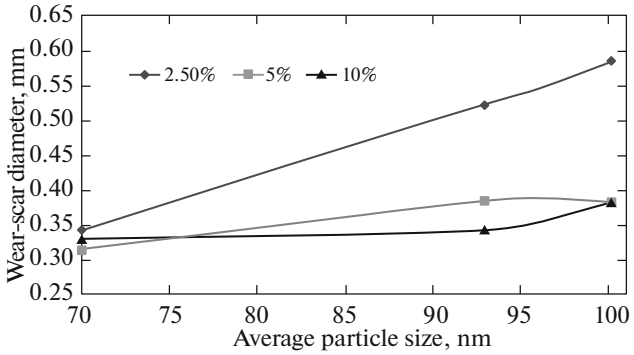


**Fig. 14.** Dependence of the wear-scar diameter on the Cu particles size.

## CONCLUSIONS

Based on the above, it is necessary to mention that the application of the metal nanoparticles, copper in particular, as the metal-cladding component being the part of the lubricant exerts a positive influence on its tribological properties; that results in the endurance improvement of the moving parts and mechanisms, which is the main aim of tribologists. Introducing nanoparticles makes it possible to fill micro- and nanoinequality quickly and effectively; this is connected with their small sizes and quite different shapes. All that results in the formation of a complex protective (so-called "servovite") film on the moving surfaces and a decrease in friction and wear.

## ACKNOWLEDGMENTS

A.A. Milov fulfilled his work in the framework of the State Assignment for 2016, no. 007-01114-16PR 0256-2014-0009.

K.A. Lomachenko expresses gratitude for Fellowship Grant from the President of the Russian Federation SP-2796.2016.1.

## REFERENCES

1. J. Ruan and B. Bhushan, "Atomic-scale and microscale friction of graphite and diamond using friction force microscopy," J. Appl. Phys. **76**, 5022–5035 (1994).
2. E. Tocha, H. Schönherr, and G. J. Vancso, "Quantitative nanotribology by AFM: a novel universal calibration platform," Langmuir **22**, 2340–2350 (2006).
3. A. S. Kuzharov, V. E. Burlakova, A. A. Kuzharov, S. B. Bulgarevich, E. E. Akimova, B. G. Konoplev, and O. A. Ageev, "Molecular mechanisms of self-organization in friction. Part VII. Fluctuations of the tribo-EMF and stepwise coagulation of copper nanoclusters

when the servovit film appears under the effect of wearlessness," J. Frict. Wear **30**, 271–276 (2009).

4. L. Rapoport, V. Leshchinsky, M. Lvovsky, I. Lapsker, Y. Volovik, and Y. Feldman, "Superior tribological properties of powder materials with solid lubricant nanoparticles," Wear **255**, 794–800 (2003).
5. F. Wang, Q. L. Bi, X. B. Wang, and W. M. Liu, Tribol. Int. **41**, 158 (2008).
6. Y. B. Guo, D. G. Wang, S. H. Liu, and S. W. Zhang, "Fabrication and tribological properties of polyelectrolyte multilayers containing in situ gold and silver nanoparticles," Colloids Surf. A: Physicochem. Eng. Asp. **417**, 1–9 (2013).
7. E. Songfeng, L. Shi, and Z. Guo, "Tribological properties of self-assembled gold nanoparticles on silicon with polydopamine as the adhesion layer," Appl. Surf. Sci. **292**, 750–755 (2014).
8. Y. Y. Wu, W. C. Tsui, and T. C. Liu, "Experimental analysis of tribological properties of lubricating oils with nanoparticle additives," Wear **262**, 821 (2006).
9. Bao-Sen Zhang, Bin-Sh. Xu, and Yi Xu, "Cu nanoparticles effect on the tribological properties of hydrosilicate powders as lubricant additive for steel-steel contacts," Tribol. Int. **44**, 883–884 (2011).
10. A. S. Kuzharov, A. A. Kuzharov, Kh. Nguen, K. G. Shuchev, and A. A. Ryzhkin, "Molecular mechanisms of self-organization under friction. Part VIII. Physicochemical and functional properties of some remetallizers on the current automobile chemistry market," J. Frict. Wear. **36**, 49–55 (2015).
11. A. S. Kuzharov, A. A. Kuzharov, Kh. Nguen, B. S. Luk'yanov, A. A. Ryzhkin, K. G. Shuchev, A. V. Soldatov, and A. A. Guda, "Physical-chemical and tribological properties of metal-cladding additives 'Nano doctor' and 'Restore'," Nanoinzhen., No. 9 (39), 19-25 (2014).
12. M. J. Frisch, G. W. Trucks, H. B. Schlegel, et al., *Gaussian 09* (Gaussian Inc., Wallingford CT, 2013).
13. V. L. Mazalova and A. V. Soldatov, J. Struct. Chem. **49**, S107 (2008).

*Translated by E. Grishina*